Experimental and numerical investigations on the ratcheting characteristics of cylindrical shell under cyclic axial loading

M. Shariati*[1], H. Hatami[1], H. Torabi[2] and H.R. Epakchi[1]

*[1]Department of Mechanical Engineering, Shahrood University of Technology,
Daneshgah Blvd, Shahrood, Semnan, Iran*
[2]Young Researchers Club, Mashhad Branch, Islamic Azad University, Mashhad, Iran

Abstract. The ratcheting characteristics of cylindrical shell under cyclic axial loading are investigated. The specimens are subjected to stress-controlled cycling with non-zero mean stress, which causes the accumulation of plastic strain or ratcheting behavior in continuous cycles. Also, cylindrical shell shows softening behavior under symmetric axial strain-controlled loading and due to the localized buckling, which occurs in the compressive stress-strain curve of the shell; it has more residual plastic strain in comparison to the tensile stress-strain hysteresis curve. The numerical analysis was carried out by ABAQUS software using hardening models. The nonlinear isotropic/kinematic hardening model accurately simulates the ratcheting behavior of shell. Although hardening models are incapable of simulating the softening behavior of the shell, this model analyzes the softening behavior well. Moreover, the model calculates the residual plastic strain close to the experimental data. Experimental tests were performed using an INSTRON 8802 servo-hydraulic machine. Simulations show good agreement between numerical and experimental results. The results reveal that the rate of plastic strain accumulation increases for the first few cycles and then reduces in the subsequent cycles. This reduction is more rapid for numerical results in comparison to experiments.

Keywords: cylindrical shell; cyclic axial loading; ratcheting; hardening model; finite element model

1. Introduction

Cylindrical shells are frequently used in the manufacturing of aircrafts, missiles, boilers, pipelines, automobiles, and some submarine structures. These shells may experience cyclic axial loading and influence the fatigue life. Earthquakes are such natural loadings which can be applied to these shells (Kulkari *et al.* 2004). One of the more essential problems which causes cylindrical shells under cyclic loading to be rarely investigated is making especial fixtures for applying the loads, thus few studies have been conducted in this field. Yoon *et al.* (2003) performed a study on stainless steel shells. They predicted the buckling strain amplitude of shells under the cyclic axial loading lower than the monotonic compression loading. Due to the problems in performing experimental tests,

*Corresponding author, Ph.D., E-mail: mshariati44@gmail.com, mshariati@shahroodut.ac.ir

theses studies have been conducted more on cylindrical shells under cyclic bending loadings which can be performed more easily (Chang 2008, Rahman *et al.* 2008, Chang *et al.* 2009, Lee 2010, Zakavi *et al.* 2010). The cyclic bending loading can lead to the non-monotonic loading distribution over the ends of shells. Bending tests can be performed to avoid those problems, as they do not require a gripping device. However, bending tests also have some shortcomings. The stress distribution in bending is not uniform throughout the cross-section and the cross-section can become distorted when large bending loads are applied (Yoon *et al.* 2003). Stress-control loading, despite non zero mean stress, may lead cyclically to accumulation of residual plastic strain in the material which is called ratcheting. These stresses should be greater than yield stress in the material. This means that the material or structures under stress should yield plastically. Ratcheting has a significant role in safety and life prediction of engineering structures (Shariati and Hatami 2011).

Jiao *et al.* (2009) performed an analysis on tubes. In this study, the effects of numbers of cycles with the mean stress and stress amplitude for specimens subjected to the constant internal pressure and cyclic axial load have been investigated. Sun *et al.* (2010) performed another numerical study on the behavior of stress-strain curve of cylindrical shells under combination of axial and torsional loads. Dong *et al.* (2006) simulated the hysteretic behaviors of channel and C-section cold-formed steel members (CFSMs) under cyclic axial loading with the finite element method (FEM). Also, axial cyclic loading causes elephant foot buckling on the constrained ends and at the bottom if the shell is vertical and constrained at the bottom (Zhang *et al.* 2008). Therefore, few works have been performed on the stress-strain behavior of cylindrical shells subjected to cyclic axial stress-controlled and strain-controlled loadings and buckling behavior of cylindrical shells (Sato and Shimazaki 2011, Shariati *et al.* 2012).

In this paper, we have studied the behavior of hysteresis curve of cylindrical shells subjected to axisymmetric axial stress-controlled and symmetric axial strain-controlled loadings. In order to use the mechanical properties for numerical simulations, simple tensile test has been performed on several standards specimens experimentally. Additionally, the existing linear kinematic hardening and nonlinear isotropic/kinematic models using the ABAQUS finite element software were carried out in order to compare results with experiment tests.

2. Numerical analysis using the FEM

The numerical simulations were carried out using the finite element software ABAQUS 6.9-1. To analyze materials which are subjected to cyclic loading, a kinematic hardening model with two parts was used, linear kinematic and nonlinear isotropic/kinematic hardening. This is the most thorough and accurate model to analyze problems under cyclic loadings (Owen and Hinton 1980, ABAQUS user manual 2009).

In the primary model, the stress value is proportional to the value of α as back stress in yield surface but, does not change. ABAQUS software uses linear Ziegler method defined according to Eq. (1) (ABAQUS user manual 2009)

$$\dot{\alpha} = C\frac{1}{\sigma^0}(\sigma_{ij} - \alpha_{ij})\dot{\bar{\varepsilon}}^{pl} + \frac{1}{c}\alpha_{ij}\dot{C} \qquad (1)$$

where C is the material constant and c is the kinematic hardening modulus. Parameters σ^0 and $\bar{\varepsilon}^{pl}$ denote the current yield stress and the equivalent plastic strain, respectively. As mentioned before,

the value of yield surface remains constant. In other words, in Eq. (1), σ^0 is always equal to $\hat{\sigma}^0$ which is equivalent to the yield stress with zero plastic strain.

The nonlinear isotropic/kinematic hardening model which is presented here was calculated by Chaboche's equations. This model contains evolution of the yield surface which is proportional to the value of α in the stress zone. Also, change of the size of the yield surface is proportional to the value of ε^{pl} as plastic strain (Chaboche *et al.* 1990). For introducing this model, a nonlinear term was added to Eq. (1) in order to show change of the size of the yield surface. Thus, the equation is given as follows, where γ is the material constant (ABAQUS user manual 2009)

$$\dot{\alpha} = C\frac{1}{\sigma^0}(\sigma_{ij} - \alpha_{ij})\dot{\bar{\varepsilon}}^{pl} - \gamma\alpha\dot{\bar{\varepsilon}}^{pl} + \frac{1}{c}\alpha_{ij}\dot{C} \tag{2}$$

where ($\cdot$) denotes the derivative with respect to time. Although, this model cannot analyze the plasticity problems in which the yield stress associated with the rate of strain, to study problems under the cyclic loading we must use this model. In order to define this model, the isotropic region (increase of the stress surface) and the kinematic region (evolution of the stress surface) should be defined separately. Increase of the stress surface was defined using σ^0 as an exponential function as follows

$$\sigma^0 = \hat{\sigma}^0 + Q_\infty(1 + e^{-b\varepsilon^{pl}}) \tag{3}$$

where Q_∞ and b are the material constants. Simple tension test was conducted to determine evolution of the stress surface. Data for σ_i and ε_i^{pl} were calculated by considering simple tensile loading part of the half cycle.

Element S8R5 was used in numerical simulation which is an eight node shell element with five degree of freedom in each node. Two ends of the cylindrical shell are bound with node bond to a rigid plate. Each rigid plate has a reference point. Reference point in the above rigid plate with boundary condition of displacement/rotation type is bound to every direction. i.e. (U1 = U2 = U3 = UR1 = UR2 = UR3 = 0). The lower reference point is bound to every direction except U3. A value is assigned to U3 parameter for displacement-control loading. Moreover, a sinus wave is allocated to amplitude parameter for periodical loading. The lower rigid point may be put under concentrated force-control loading and loading in CF1 and CF2 directions are zero and a value would be assigned to CF3 parameter. Furthermore, in this loading, like displacement-control loading, from amplitude parameter may be used for periodical loading.

2.1 Geometry and mechanical properties

In this study, the cylindrical shell with length ($L = 125$ mm), upper diameter ($D = 42$ mm), and thickness ($t = 0.85$ mm) under the stress-controlled loading was analyzed. Furthermore, experimental tests were conducted on the cylindrical shell with length ($L = 195$ mm), and the same thickness and upper diameter subjected to the symmetric axial strain-controlled loading.

The cylindrical shells used for this study were made of St37. The mechanical properties of this steel alloy were determined according to ASTM E8 standard (ASTM A 370-05 2005), using the INSTRON 8802 servo hydraulic machine (Fig. 1).

The stress-strain curve and respective values are shown in Fig. 2. Based on the linear portion of stress-strain curve, the value of elastic modulus was computed as $E = 210$ GPa and the value of

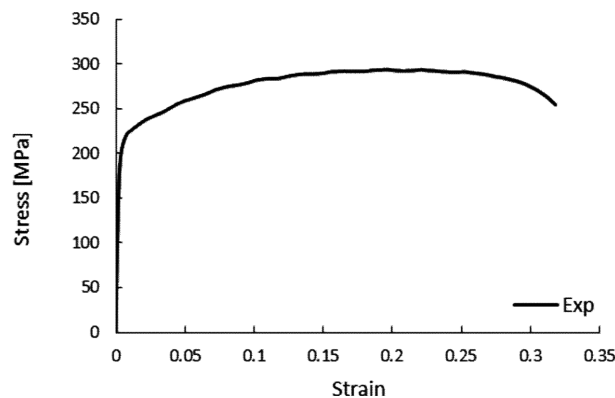Fig. 1 Simple tension test according to ASTM E8 standard

Fig. 2 Stress-strain curve

yield stress was obtained as σ_y = 198 MPa. Furthermore, the value of Poisson's ratio was assumed to be ν = 0.3.

2.2 Boundary conditions

To apply cyclic axial loadings to cylindrical shells a fixture which could tolerate compressive and tensile loads without any sliding movement was needed. Since the shells were thin, we could not make thread on both ends of them. Thus, structures were used to strengthen both ends of shells as shown in Fig. 3(a). These structures were threaded and welded to both ends of the cylindrical shells to prevent the separation of shells and structures during loading. Examples of these structures for cyclic axial loading can be seen in the paper of Nip *et al.* (2010). Fig. 3(b) shows fixtures which were used to fasten the specimens to the fixed and moving steel sleeve fixtures of INSTRON machine inserted at both ends which mimics the fixed–fixed boundary condition used in the finite element simulations (Fig. 4).
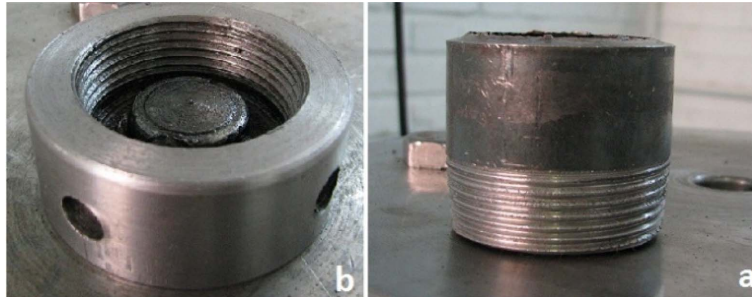
Fig. 3 (a) Structure used to strengthen both ends of cylindrical shell, (b) fixture
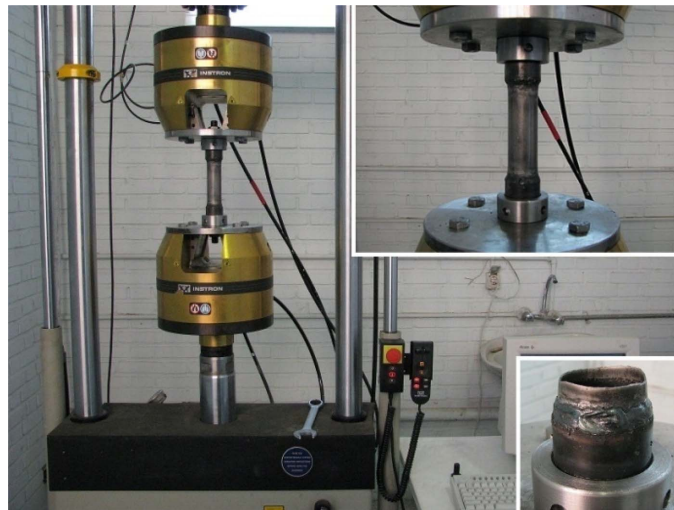

Fig. 4 A servo hydraulic INTSRON 8802 machine in stress-controlled loading on cylindrical shell

3. Experimental tests

Experimental tests were conducted on specimens in order to confirm the numerical results. For these tests, a servo-hydraulic INSTRON 8802 machine was used (Fig. 4).

In order to obtain the ratcheting behavior of cylindrical shells, the specimens were subjected to the constant mean stress of 96 MPa and the stress amplitude of 146 MPa. With increasing the stress amplitude the rate of plastic strain accumulation increases and the ratcheting becomes more visible. But, as the specimens were cylindrical shell, they would buckle in compression. In order to prevent the effect of buckling on the ratcheting behavior of shells low range of stress amplitude was used. In addition, with increasing the mean stress, failure will occur sooner; therefore the value of mean stress was chosen so that failure occurs at the higher number of cycles. Moreover, selecting smaller mean stress and stress amplitude will stop the ratcheting strain of the cylindrical shell in subsequent cycles (Kulkarni *et al.* 2003).

The stress-strain curve recorded in this kind of loading is shown in Fig. 5. At higher cycles as the load reaches the maximum value of tensile stress close to the both ends of specimen, necking
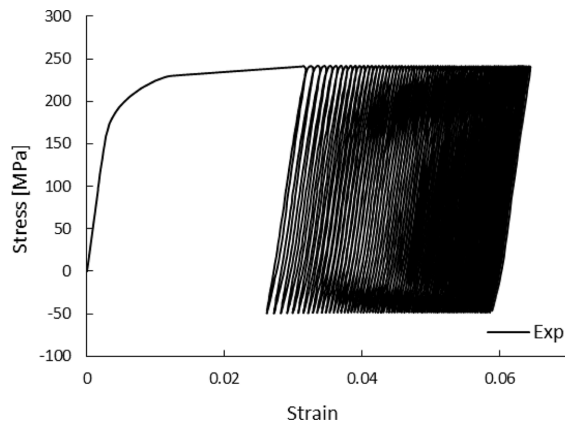
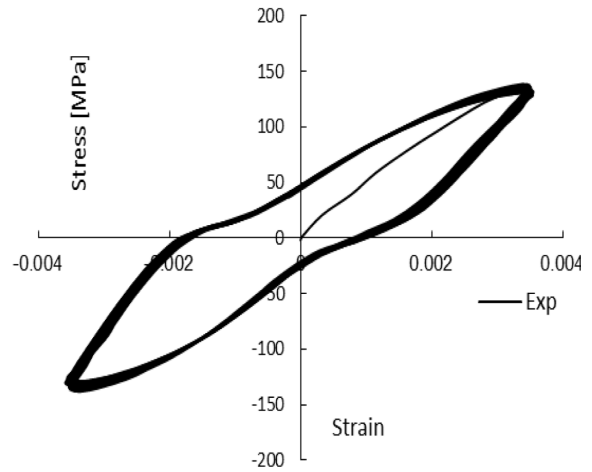Fig. 5 Ratcheting behavior of cylindrical shell under stress controlled loading with a non-zero mean stress

Fig. 6 Softening behavior of cylindrical shell under symmetric axial strain controlled loading

occurs and the plastic strain accumulation will lead to the failure of shell in subsequent cycles.

In order to study the softening and hardening behavior of cylindrical shells, the specimens were subjected to strain-controlled loading with the strain amplitude of 0.0037. Furthermore, to prevent relaxation behavior of the shell, symmetric loading with zero mean strain was applied to it (Boller *et al.* 1987). The stress-strain curve recorded in this kind of loading is shown in Fig. 6. Stress behavior is the same in tension and compression, thus Von Mises yield criterion can be used in the numerical simulation (ABAQUS user manual 2009).

4. Confirmation of numerical results with experimental findings

The experimental stress-strain results for the first five cycles of axisymmetric axial stress-controlled loading in comparison to numerical results are presented in Fig. 7. As shown in this figure, the finite element solution compares well with the experimental data, and the ratcheting behavior from the numerical simulation is visible well.

Increasing the mean stress will lead to the increase of plastic strain. Thus, the shell reaches failure sooner. The rate of plastic strain accumulation reduces faster for the numerical simulation in comparison to the experimental results (Fig. 8). The cumulative errors after 10, 20 and 30 cycles are %5, %10 and %14, respectively. By approaching the zero mean stress, the plastic strain accumulation becomes stable after a few cycles.

Among the existing hardening models in ABAQUS software, the nonlinear isotropic/kinematic hardening model with von Mises yield criterion is the only one that can model the ratcheting behavior of shells. Two other hardening models, isotropic hardening model and linear kinematic hardening model, are used in this software separately which cannot simulate the ratcheting of shell and as a result a closed loop without the ratcheting will be obtained. Because in isotropic hardening model only the extent of yield surface would change in stress space and in linear kinematic hardening model only the center of yield surface would move. Thus, these two models would only
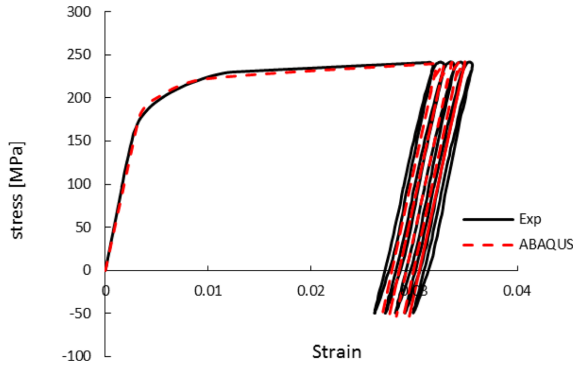
Fig. 7 Comparison of experimental and numerical results for ratcheting behavior of cylindrical shell
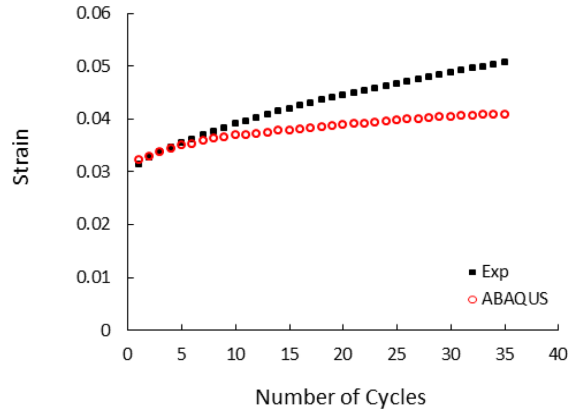

Fig. 8 Comparison of experimental and numerical strain values for maximum stress in each cycle
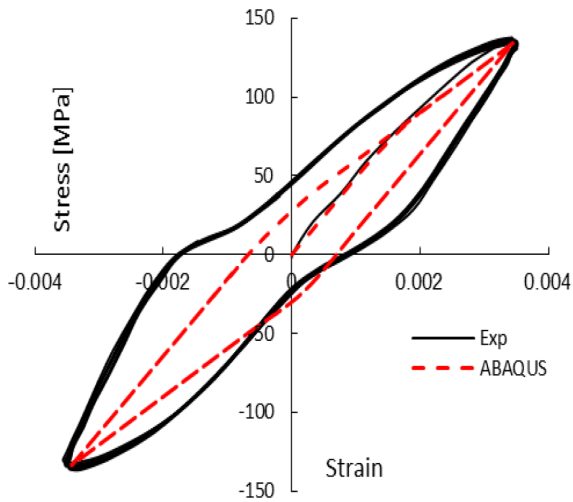

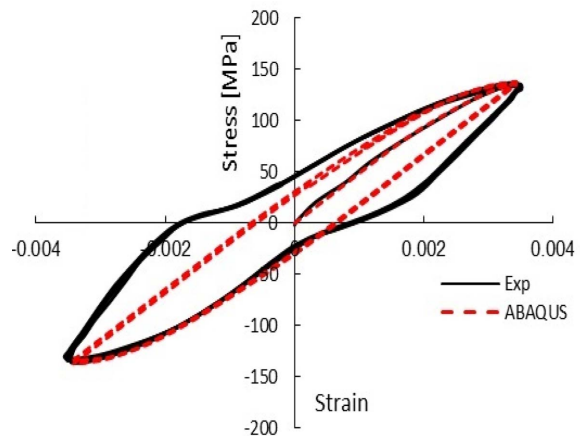Fig. 9 Comparison of experimental results and the kinematic hardening model

Fig. 10 Comparison of experimental results and nonlinear isotropic/kinematic hardening model

simulate closed loops.

For the first few cycles a good correlation between numerical and experimental results can be observed. However, then as the applied mean stress on the shell is chosen to increase the number of cycles to failure, the ratcheting behavior reaches a stable level faster. This difference is smaller for higher mean stresses.

The behavior of non-loading regions of numerical and experimental results has an acceptable correlation. Considering the nonlinear characteristics of curves in non-loading regions, the numerical method has simulated these characteristics accurately. In order to prevent buckling of shells, specific stress amplitude was selected. Therefore, the loading and unloading curves are well matched and finally for the maximum tensile stress in each cycle, the plastic strain increases in the shell.
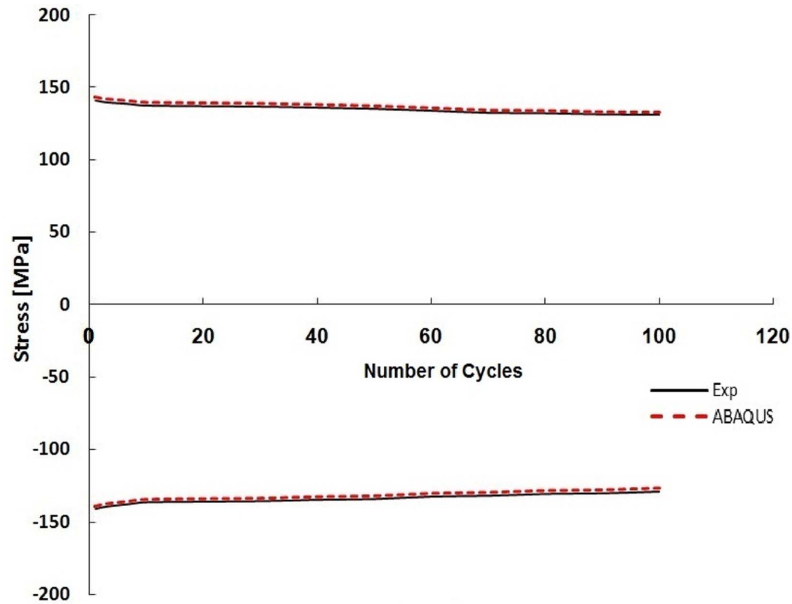
Fig. 11 Comparison of the experimental maximum tensile and compressive stress and the nonlinear isotropic/
        kinematic model

Fig. 9 shows comparison of experimental stress-strain results under the symmetric axial strain-controlled loading and the linear kinematic model. As the center of yield surface was transferred in the stress region, this model is incapable of simulating the softening behavior of the shell.

Considering the nonlinear isotropic/kinematic hardening model, the yield area in stress region changes in all directions monotonically and its center is also transferred. Therefore, a good correlation is observed between numerical simulation and experimental results, as shown in Fig. 10. This figure shows the softening behavior model and increase of the residual plastic strain in continuous cycles. The residual plastic strain in the tensile region and experimental results are well matched.

Fig. 11 reveals the softening behavior of the shell subjected to the symmetric axial strain-controlled loading in the first few cycles. However, the rate of softening is reduced in subsequent cycles and then reaches a stable value. The maximum error between numerical and experimental results is %2 and occurs at the maximum stress. Also, in the hysteresis curve the error of residual plastic strain is %5 at the tensile region.

5. Conclusions

The axial cyclic stress-strain characteristics of cylindrical shells were investigated experimentally. Specimens subjected to the stress-controlled loading with none zero mean stress shows ratcheting characteristics. The plastic strain accumulation is continued till failure occurs in continuous cycles. The rate of plastic strain accumulation increases in the first cycles and then reduces in subsequent cycles.

The existing nonlinear isotropic/kinematic hardening model in ABAQUS software simulates well the ratcheting characteristic of cylindrical shells and matches well with the experimental results. The plastic strain accumulation simulated by this model is smaller than the experimental results.

Specimens subjected to the symmetric strain-controlled loading shows softening behavior. Due to the occurrence of localization buckling in the shell, the residual plastic strain is more in the compressive region in comparison to the tensile region. This value of residual plastic strain increases each cycle. The rate of softening is high in the first few cycles, reduces in subsequent cycles and finally, the softening behavior becomes stable. Additionally, the linear kinematic model cannot simulate the softening behavior of a shell but, the nonlinear isotropic/kinematic model simulates the softening behavior well.

References

ABAQUS Analysis User's Manual (2009), v6.9.1 Section 19.2.2: Models for Metals Subjected to Cyclic Loading.

ABAQUS Theory Manual (2009), v6.9.1 Section 4.3.5: Models for Metals Subjected to Cyclic Loading.

ASTM A370-05, Standard Test Methods and Definitions for Mechanical Testing of Steel Products.

Boller, C. and Seeger, T. (1987), *Materials Data for Cyclic Loading*, Amsterdam, Elsevier.

Chang, K.H., Pan, W.F. and Lee, K.L. (2008), "Mean moment effect on circular thin-walled tubes under cyclic bending", *Struct. Eng. Mech.*, **28**(5), 495-514.

Chang, K.H. and Pan, W.F. (2009), "Buckling life estimation of circular tubes under cyclic bending", *Int. J. Solids Struct.*, **46**(2), 254-270.

Chaboche, J.L. and Lemaitre, J. (1990), *Mechanics of Solid Materials*, Cambridge University Press.

Dong, J., Wang, S. and Lu, X. (2006), "Simulations of the hysteretic behavior of thin-wall cold-formed steel members under cyclic uniaxial loading", *Struct. Eng. Mech.*, **24**(3), 323-337.

Jiao, R. and Kyriakides, S. (2009), "Ratcheting, wrinkling and collapse of tubes under axial cycling", *Int. J. Solids Struct.*, **46**(14-15), 2856-2870.

Kulkarni, S.C., Desai, Y.M., Kant, T., Reddy, G.R., Parulekar, Y. and Vaze, K.K. (2003), "Uniaxial and biaxial ratchetting study of SA333 Gr.6 steel at room temperature", *Int. J. Press. Vessel. Pip.*, **80**, 179-185.

Kulkarni, S.C., Desai, Y.M., Kant, T., Reddy, G.R., Prasad, P., Vaze, K.K. and Gupta, C. (2004), "Uniaxial and biaxial ratchetting in piping materials—experiments and analysis", *Int. J. Press. Vessel. Pip.*, **81**, 609-617.

Lee, K.L. (2010), "Mechanical behavior and buckling failure of sharp-notched circular tubes under cyclic bending", *Struct. Eng. Mech.*, **34**(3), 367-376.

Nip, K.H., Gardner, L. and Elghazouli, A.Y. (2010), "Cyclic testing and numerical modelling of carbon steel and stainless steel tubular bracing members", *Eng. Struct.*, **32**, 424-441.

Owen, D.R.J. and Hinton, F. (1980), *Finite Elements in Plasticity – Theory and Practice*, Pineridge Press Ltd.

Rahman, S.M., Hassan, T. and Corona, E. (2008), "Evaluation of cyclic plasticity models in ratcheting simulation of straight pipes under cyclic bending and steady internal pressure", *Int. J. Plast.*, **24**, 1756-1791.

Sato, M. and Shimazaki, K. (2011), "Approximate formulation for bifurcation buckling loads of axially compressed cylindrical shells with an elastic core", *Int. Multis. Mech.*, **4**(4), 313-320.

Shariati, M. and Hatami, H. (2012), "Experimental study of SS304L cylindrical shell with/without cutout under cyclic axial loading", *Theo. Appl. Fract. Mech.*, **58**, 35-43.

Shariati, M., Hatami, H., Yarahmadi, H. and Eipakchi, H.R. (2011), "An experimental study on the ratcheting and fatigue behavior of polyacetal under uniaxial cyclic loading", *Mater. Des.*, **34**, 302-312.

Sun, G.Q. and Shang, D.G. (2010), "Prediction of fatigue lifetime under multiaxial cyclic loading using finite element analysis", *Mater. Des.*, **31**(1), 126-133.

Yoon, S., Hong, S.G., Lee, S.B. and Kim, B.S. (2003), "Low cyclic fatigue testing of 429EM stainless steel pipe", *Int. J. Fatigue*, **8**(9-11), 1301-1307.

Zakavi, S.J., Zehsaz, M. and Eslami, M.R. (2010), "The ratchetting behavior of pressurized plain pipework subjected to cyclic bending moment with the combined hardening model", *Nucl. Eng. Des.*, **240**, 726-737.

Zhang, C., Liu, Y. and Goto, Y., (2008), "Plastic buckling of cylindrical shells under transverse loading", *Tsinghua Sci. Technol.*, **13**, 202-210.